Receptor Conformations Involved in Dopamine D$_{2L}$ Receptor Functional Selectivity Induced by Selected Transmembrane-5 Serine Mutations^S

J. Corey Fowler, Supriyo Bhattacharya, Jonathan D. Urban, Nagarajan Vaidehi, and Richard B. Mailman

Department of Pharmacology, Pennsylvania State University College of Medicine, Hershey Pennsylvania (R.B.M.); Division of Medicinal Chemistry and Toxicology Curriculum, University of North Carolina School of Medicine, Chapel Hill, North Carolina (J.C.F., J.D.U., R.B.M.); and Beckman Research Institute at City of Hope Medical Center, Duarte, California (S.B., N.V.)

ABSTRACT

Although functional selectivity is now widely accepted, the molecular basis is poorly understood. We have studied how aspects of transmembrane region 5 (TM5) of the dopamine D$_{2L}$ receptor interacts with three rationally selected rigid ligands (dihydrexidine, dinapsoline, and dinoxyline) and the reference compounds dopamine and quinpirole. As was expected from homology modeling, mutation of three TM5 serine residues to alanine (S5.42A, S5.43A, S5.46A) had little effect on antagonist affinity. All three mutations decreased the affinity of the agonist ligands to different degrees, S5.46A being somewhat less affected. Four functions [adenylate cyclase (AC), extracellular signal-regulated kinase 1/2 phosphorylation (MAPK), arachidonic acid release (AA), and guanosine 5′-O-(3-thio)triphosphate binding (GTPγS)] were assessed. The intrinsic activity (IA) of quinpirole was unaffected by any of the mutations, whereas S5.42A and S5.46A mutations abolished the activity of dopamine and the three rigid ligands, although dihydrexidine retained IA at MAPK function only with S5.42A. Remarkably, S5.43A did not markedly affect IA for AC and MAPK for any of the ligands and eliminated AA activity for dinapsoline and dihydrexidine but not dinoxyline. These data suggest that this mutation did not disrupt the overall conformation or signaling ability of the mutant receptors but differentially affected ligand activation. Computational studies indicate that these D$_2$ agonists stabilize multiple receptor conformations. This has led to models showing the stabilized conformations and interhelical and receptor-ligand contacts corresponding to the different activation pathways stabilized by various agonists. These data provide a basis for understanding D$_{2L}$ functional selectivity and rationally discovering functionally selective D$_2$ drugs.

Introduction

Functional selectivity is the phenomenon by which the binding of a ligand to a receptor results in markedly different levels of activation (or lack thereof) of one or several of the signaling pathways linked to the targeted receptor. Although this signaling bias runs counter to classic concepts of drug-receptor mechanisms, it has become firmly established and has been demonstrated for dozens of receptors (Urban et al., 2007; Neve, 2009). As well as being heuristically interesting, it is also generally appreciated that functionally selective ligands with the "correct" bias may yield improved therapeutic indices versus drugs that are "typical" agonists or antagonists (Mailman, 2007). It is generally believed that the functionally selected properties of a ligand are a result of the differential stabilization and/or induction of active states of the target receptor that are associated with specific signaling pathways (Kenakin, 1995, 2007; Urban et al., 2007). However, there has been little exploration of how this may occur.

ABBREVIATIONS: CHO, Chinese hamster ovary; DNS, dinapsoline; AC, adenylate cyclase; AA, arachidonic acid release; MAPK, mitogen-activated protein kinase; AA, arachidonic acid; DNX, dinoxyline; DHX, dihydrexidine; DA, dopamine; GPCR, G protein-coupled receptor; PMSF, phenylmethylsulfonyl fluoride; TM,transmembrane; WT, wild type; GTPγS, guanosine 5′-O-(3-thio)triphosphate; BSA, bovine serum albumin; PBS, phosphate-buffered saline; n_H, Hill coefficient; $K_{0.5}$, apparent affinity constant ($n_H < 1.0$), equals K_I when $n_H = 1$; HD$_{2L}$, human dopamine D$_{2L}$ receptor; BE, binding energy; HB, hydrogen bond; PDB, protein data bank; ANOVA, analysis of variance.

One of the earliest demonstrations of functional selectivity was with the dopamine D_2 receptor (Lawler et al., 1994, 1999). In particular, studies with a series of relatively rigid, conformationally restrained D_2 ligands showed extreme bias in signaling, in some cases as extreme as full agonist and pure antagonist (Mottola et al., 1991, 2002; Kilts et al., 2002; Gay et al., 2004). Thus, in Chinese hamster ovary (CHO) cells expressing hD_{2L} receptors, Gay et al. (2004) reported that dinapsoline (DNS) was a full agonist at several functions [e.g., fully inhibiting cAMP accumulation (AC) and fully stimulating p44/p42 MAP kinase phosphorylation (MAPK)] yet was a partial agonist at stimulating G protein-coupled inward rectifying potassium channels. Conversely, dinoxyline (DNX) was a full agonist at all four effector pathways (Gay et al., 2004). These data are noteworthy because there are only subtle differences in the chemical structures of DNS and DNX (see Fig. 1).

Subtle structural difference in a ligand may lead to functional selectivity (Gay et al., 2004; Ryman-Rasmussen et al., 2005). Thus, we hypothesized that modification of the D_{2L} receptor in regions where such ligands bind could be informative about the manner by which functionally selective signaling occurs. The current experiments address this hypothesis by studying the role of specific binding interactions that occur between the D_{2L} receptor and three rigid analogs, dihydrexidine (DHX) (Lovenberg et al., 1989), DNS (Ghosh et al., 1996), and DNX (Grubbs et al., 2004). These ligands were originally designed as novel D_1 agonists in which the accessory phenyl ring was expected to confer both high D_1 affinity and high D_1:D_2 selectivity (Nichols, 1983; Charifson et al., 1989; Mottola et al., 1996). All three compounds also unexpectedly had significant D_2 affinity, leading to the discovery of D_2 functionally selective signaling for DHX and DNS (Kilts et al., 2002; Mottola et al., 2002; Gay et al., 2004).

In the current study, computational approaches were used to hypothesize specific binding interactions within each ligand-receptor complex. The affinity and functional properties of the probe and reference ligands was then assessed using four distinct functional endpoints. The resulting data are consistent with the hypothesis that subtle changes in ligand-specific interactions induced by mutation of selected amino acids of the receptor may stabilize and/or induce certain receptor conformations that lead to functional selectivity (i.e., differential activation of one or more signaling pathways).

Materials and Methods

Materials

Dinapsoline [(+)8,9-dihydroxy-2,3,7,11b-tetrahydro-1H-napth[1,2,3-de]isoquinoline], dinoxyline [(+)8,9-dihydroxy-1,2,3,11b-tetrahydrochromeno[4,3,2,-de]isoquinoline], and dihydrexidine [trans-10,11-dihydroxy-5,6,6a,7,8,12b-hexahydrobenzo[a]phenanthridine] were synthesized according to published procedures (Brewster et al., 1990; Ghosh et al., 1996; Grubbs et al., 2004). Dopamine, quinpirole, 3-isobutyl-1-methylxanthine, EDTA, dithiothreitol, sucrose, pepstatin A, leupeptin, PMSF, fetal bovine serum, and other standard chemical reagents were purchased from Sigma-Aldrich (St. Louis, MO) and Sigma/RBI (Natick, MA). [^{3}H]N-methylpiperone, [^{3}H]arachidonic acid (or [5,6,8,9,11,12,14,15-^{3}H(N)]AA), and [^{35}S]GTPγS were purchased from Amersham Biosciences Inc. (Chalfont St. Giles, Buckinghamshire, UK). ^{125}I for cAMP assays was purchased from PerkinElmer Life and Analytical Sciences (Waltham, MA), and processed as described by Brown et al. (2009). cAMP primary antibody was obtained from Dr. Gary Brooker (George Washington University, Washington DC); secondary antibody, rabbit anti-goat IgG, was purchased from Advanced Magnetics (Cambridge, MA). HEPES buffer was purchased from Research Organics (Cleveland, OH). Ham's F-12, Opti-MEM, penicillin, streptomycin, primers, and lipofectamine were purchased from Invitrogen (Carlsbad, CA). Hygromycin B was purchased from Roche Applied Science (Indianapolis, IN). Primary antibody to phospho-p44/p42 MAPK and secondary antibody, anti-rabbit horseradish peroxidase-conjugated, were purchased from Cell Signaling Technology Inc. (Danvers, MA).

Molecular Biology and Cell Culture

CHO hD_{2L} wild-type and mutant cells were maintained in Ham's F-12 media supplemented with 10% fetal bovine serum, 100× penicillin-streptomycin, and 100 μg/ml hygromycin. Mutant cell lines were constructed using the pcDNA5/FRT plasmid obtained from Invitrogen. After subcloning of the hD_{2L} receptor into the plasmid, point mutations were introduced using standard polymerase chain reaction techniques. Stable transfections of point mutants into CHO K1 cells were conducted using modifications of a previously published protocol (Milligan, 1999). Throughout this article, the identification of the mutated amino acid residue will be made using universal notation proposed by Ballesteros and Weinstein (1995) in which the first number denotes the TM helix in which the residue is
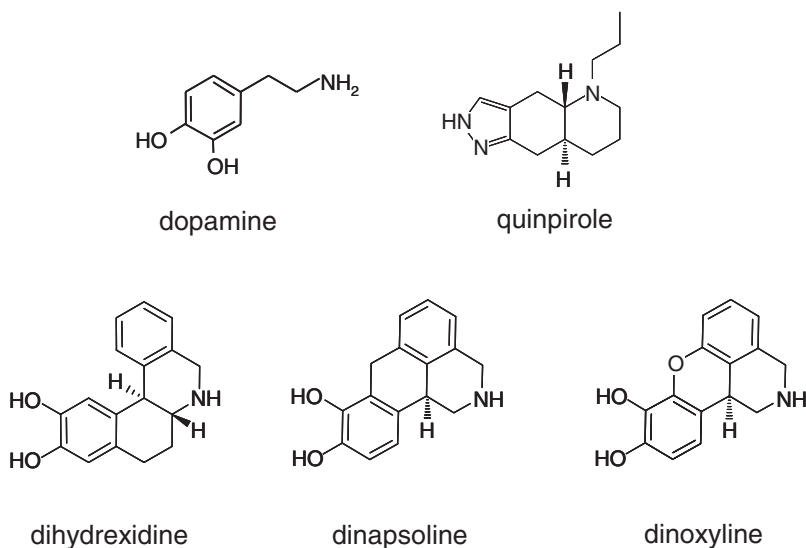

dopamine   quinpirole

dihydrexidine   dinapsoline   dinoxyline

Fig. 1. Structures of probe ligands used in this study.

located, and the second number pair is the location of the residue under question relative to the most conserved residue for that helix. The residues we studied (listed in both universal notation and absolute position) were S5.42A (S193A), S5.43A (S194A), and S5.46A (S197A).

Radioreceptor Assays

Membranes for radioreceptor assays were prepared by rinsing cells with phosphate-buffered saline and then lysing with a solution containing 2 mM HEPES, 2 mM EDTA, 1 mM dithiothreitol, 1 μg/ml pepstatin A, 0.5 μg/ml leupeptin, and 0.05 μg/ml PMSF. Cell fragments were scraped, homogenized, and centrifuged at 30,000g for 30 min. After centrifugation, cell pellets were resuspended, homogenized, and placed into storage buffer (50 mM HEPES, 0.32 M sucrose, 1 μg/ml pepstatin A, 0.5 μg/ml leupeptin, and 0.05 μg/ml PMSF) and stored at $-80°$C. Saturation binding assays were conducted using protocols described previously (Gay et al., 2004) but with varying concentrations of [³H]N-methyl-spiperone to determine the B_{max} and K_D for each membrane preparation (e.g., hD$_{2L}$ WT, hD$_{2L}$ S5.42A, etc.). Domperidone (10 μM) was used to define nonspecific binding. Competition binding assays also used [³H]N-methyl-spiperone.

Because these experiments incorporated detailed functional analysis including GTPγS activation, we did not make use of a nonhydrolyzable GTP analog such as Gpp(NH)p to estimate the proportion of receptors that were G protein-coupled. In retrospect, this might have been useful and should be considered in future testing of the hypotheses outlined under *Discussion*.

GTPγS Assay

Measurement of [³⁵S]GTPγS binding was determined as described previously (Shapiro et al., 2003), with nonspecific binding defined by 10 μM unlabeled GTPγS. Assay tubes contained 150 to 200 pM [³⁵S]GTPγS, binding buffer (50 mM HEPES, 100 mM NaCl, 4 mM MgCl$_2$, 1 mM EDTA, 0.1% BSA, 0.1% ascorbic acid, pH adjusted to 7.4 with NaOH), 10 μM GDP, and various concentrations of agonists and/or antagonist. Membranes (approximately 100 μg protein/ml) were incubated with test compounds for 15 min at 30°C before addition of [³⁵S]GTPγS. After an additional 30-min incubation, the assay was terminated by filtration (Packard Filtermate 190 harvester; PerkinElmer Life and Analytical Sciences) with ice-cold wash buffer (50 mM HEPES and 4 mM MgCl$_2$, pH adjusted to 7.4 with KOH), and radioactivity quantified by liquid scintillation spectrometry (Packard TopCount NXT; PerkinElmer Life and Analytical Sciences).

cAMP Accumulation Assay

Measurement of dopamine receptor agonist inhibition of forskolin-stimulated cAMP accumulation was performed in whole-cell preparations as described previously (Gay et al., 2004). In brief, CHO cells were seeded in 24-well plates at a density of 2.5×10^6 cells/well, and grown for 48 h in Ham's F-12 media supplemented with 10% fetal bovine serum and 100$\times$ penicillin-streptomycin. Cells were preincubated for 5 min before in fresh media (serum-free media containing 25 mM HEPES, 500 μM 3-isobutyl-1-methylxanthine, and 0.1% ascorbic acid) at 37°C. Assay medium then was aspirated, and fresh assay medium containing forskolin and/or various concentrations of the test compounds were added. The plates were incubated for 15 min at 37°C, and cells were rinsed with fresh assay medium and then aspirated; the reaction was halted using 0.1 N HCl. The cAMP was quantified using a modified radioimmunoassay described previously (Harper and Brooker, 1975).

MAPK Assay

Measurement of dopamine receptor agonist stimulation of p44/p42 MAPK was performed in whole cell preparations by modifying a previously published protocol (Versteeg et al., 2000). CHO cells were

seeded in 96-well plates at a density of 5×10^6 cells/well and grown for 48 h in Ham's F-12 media supplemented with 10% fetal bovine serum at 37°C. Cells were serum-starved for 6 h before stimulation. Appropriate drug dilutions of the test compounds were added to each well at a volume of 100 μl for 10 min. The reaction then was terminated, and the cells fixed by aspirating the wells and adding 100 μl of 4% formaldehyde PBS solution for 20 min. Cells were washed three times with 100 μl of wash buffer (0.1% Triton X-100/PBS solution), followed by a 20-min incubation with 0.6% H$_2$O$_2$ Triton/PBS solution to quench endogenous peroxidases. After washing the cells three times again with wash buffer, and after a 1-h incubation with 10% BSA in Triton/PBS solution (to block nonspecific antibody binding), cells were incubated overnight (approximately 12 h) with a 1:250 dilution of PhosphoPlus p44/42 primary antibody (Cell Signaling Technology) in the Triton/PBS solution (100 μl) containing 5% BSA at 4°C. Cells were washed three times with wash buffer for 5 min and then incubated with 100 μl of horseradish peroxidase-conjugated goat anti-rabbit secondary antibody (1:100 dilution) with 5% BSA at room temperature for 1 h. Again, cells were washed three times with wash buffer for 5 min and then twice with PBS. Cells were then incubated with 50 μl of an o-phenylenediamine solution (0.4 mg/ml o-phenylenediamine, 17.8 mg/ml Na$_2$HPO$_4$·7H$_2$O, 7.3 mg/ml citric acid, and 0.015% H$_2$O$_2$) for 15 min at room temperature in the dark. The reaction was terminated by the addition of 25 μl of 1 M H$_2$SO$_4$ that causes a light- to dark-orange color change (A_{490}–A_{650}) that is proportional to phosphorylation.

Arachidonic Acid Assay

Measurement of dopamine receptor agonist potentiation of ATP-stimulated [³H]AA release was measured in whole-cell preparations using modifications of a previously published method (Berg et al., 1998). CHO cells were seeded in 24-well plates at a density of 5×10^5 cells/well and grown for 24 h in Ham's F-12 media supplemented with 10% fetal bovine serum at 37°C. Cells are serum-starved with 500 μl of serum-free Ham's F-12 containing 0.5 μCi/ml [³H]AA for 5 h at 37° C. Ten-microliter aliquots were removed to compare with the original triturated loading media to determine the time course and total cellular uptake of [³H]AA. Cells were washed three times for 5 min each with Hanks' balanced salt solution containing 0.5% fatty acid-free BSA and antagonists for respective wells (500 μl/well/wash). Cells then were incubated with agonists for 15 min with or without ATP dissolved in Hanks' balanced salt solution/BSA (ATP being added last and in timed increments of 5 s between wells).

Data and Statistical Analysis

Data were analyzed using Prism 4.0/5.0 (GraphPad Software, San Diego CA). Saturation analysis was conducted using a one-site binding model (Prism). Competition data used nonlinear regression and a sigmoidal equation to determine IC$_{50}$ and E_{max} values. The IC$_{50}$ values were corrected for radioligand concentration and are reported as corrected affinity values ($K_{0.5}$) adjusted by the Cheng-Prusoff equation for bimolecular interactions (Cheng and Prusoff, 1973) regardless of Hill coefficient (n_H). Intrinsic activity and potency estimates were made from sigmoidal fits of dose response data using Prism. Statistical analyses were conducted using SigmaStat 2.03 (Systat Software, Inc., San Jose, CA) or Instat 3 (GraphPad Software), using algorithms specified with each experiment.

Computational Strategy

Homology Model of Human D$_{2L}$ Receptor. The human D$_{2L}$ was modeled using three closely related GPCR crystal structures as templates: the β_2-adrenergic receptor (PDB ID: 2RH1); dopamine D$_3$ receptor (PDB ID: 3PBL); and bovine rhodopsin (PDB ID: 1GZM). Because of the distant homology and different transmembrane packing compared with the biogenic amine receptor crystals, the adenosine receptor was not used as a template for modeling the D$_{2L}$. The disulfide-bonded cystines between extracellular loop 2 and TM3 were

identified from sequence alignment with other class A GPCRs. The homology model was predicted using the software MODELLER (http://salilab.org/modeller/) (Fiser and Sali, 2003), followed by optimization of polar residues and energy minimization.

Ligand Docking. The agonist structures were modeled using the SCHRODINGER Maestro interface (Schrodinger LLC, Portland, OR). The ligand structures were optimized, and partial changes were calculated (QM, basis set 6-31G**) using the software Jaguar (Schrodinger LLC). Multiple conformations of the ligands were generated using Monte Carlo sampling (Macromodel, Maestro; Schrodinger LLC), and these conformations were docked into the D_{2L} receptor model using Glide standard precision module of Maestro. During docking, the van der Waals radii of both ligands and the receptor were scaled by 0.5 to increase diversity of the docked poses. The resulting ligand poses were clustered, and the top-ranking pose from each cluster was chosen based on binding energy. The final bound pose for each agonist was selected from these top ranking poses by visual inspection.

Ligand-Induced Receptor Conformational Changes. The ligand-induced receptor conformational change method has been discussed in detail previously (Bhattacharya et al., 2008b, 2010). Here we detail the steps of the method as applied to hD_{2L}. We identified that TM helices 3, 5, and 6 are in direct contact with all the agonists and hence would undergo conformational changes as a result of ligand binding. We performed simultaneous systematic spanning of the rotational orientation of TM helices 3, 5, and 6 in 10° increment with respect to the initial state. Although TM3, TM6 were rotated ±50°, TM5 was rotated from −50° to +20°. This process generated 968 receptor conformations. For each conformation, the following steps were performed.

- Optimization of all side-chain conformations using SCWRL 3.0 (http://dunbrack.fccc.edu/scwrl4/SCWRL4.php) (Canutescu and Dunbrack, 2003).
- Conjugate gradient minimization of the potential energy of the ligand in the field of the rest of protein fixed until convergence of 0.3 kcal/mol-Å root-mean-square deviation in force per atom is achieved.
- Calculation of the ligand binding energy, defined as the difference of the potential energy of the ligand with protein fixed and the potential energy of the free ligand calculated in water using Generalized Born solvation method (Zamanakos, 2001).
- Interhelical and ligand-receptor hydrogen bonding using HB-PLUS 3.0 (http://www.biochem.ucl.ac.uk/bsm/hbplus/) (McDonald and Thornton, 1994). This generates a three dimensional binding energy landscape in the rotational degrees of freedom of TMs 3, 5, and 6.
- Identification of all the local minima in this landscape and sorting of them by total number of interhelical hydrogen bonds (HB) and ligand-receptor HB and then by binding energy. The final ligand stabilized receptor structural model was selected based on low binding energy and high number of HBs.

Results

Ligand Rationale. For these studies, we compared the actions of the endogenous ligand dopamine and the prototypical D_2 agonist quinpirole with those of DHX, DNS, and DNX. The D_2 functional selectivity of dihydrexidine in vitro is consistent with both its D_2 functional selectivity in situ (Kilts et al., 2002; Mottola et al., 2002) and its lack of amphetamine-like behavioral actions (Darney et al., 1991), despite being a full D_1 and D_2 agonist at the canonical signaling pathway. Of particular importance for the present study is the fact that dihydrexidine has a fused ring structure with no rotatable bonds. This relatively rigid structure decreases the degrees of freedom in interpreting data of the type this study was designed to generate. The second important ligand used was dinapsoline, another rigid compound that also has been shown to have functionally selective properties with the D_2 wild-type receptor (Gay et al., 2004). The third related ligand was dinoxyline, a compound that differs from dinapsoline only in an ether-methylene bridge substitution, a feature hypothesized to influence receptor interactions in subtle, but meaningful, ways. The structures of the eutomers of these compounds are shown in Fig. 1. In all cases, the D_2 affinity of the distomer is at least 100-fold less than the eutomer at the wild-type D_2 receptor, and because of limited or unavailability of pure eutomer, racemic mixtures were used for this research. The reported $K_{0.5}$ values are based on the concentration of the racemate and were not corrected for the effects of the distomer. The synthetic ligands had no functional effect in any of these assays performed in wild-type CHO K1 cells not containing the D_{2L} receptor. The D_2 antagonist domperidone (10 μM) was tested against WT and all receptor mutants; as expected, no functional activation was seen at any endpoint tested. Domperidone completely blocked quinpirole activation of all effector endpoints with both WT and mutant receptors.

Effect of S5.42A, S5.43A, and S5.46A Mutants on Receptor Expression and Antagonist Radioligand Binding. On the basis of the large body of data for aminergic GPCRs and of the D_2 receptor that elucidated many aspects of the role of TM5 serines in interaction with ligands (Strader et al., 1989; Cox et al., 1992; Mansour et al., 1992; Woodward et al., 1996; Wiens et al., 1998; Shi and Javitch, 2002), we chose to explore the effects of the TM5 serine residues Ser5.42, Ser5.43, and Ser5.46 on the functional efficacy of the above-mentioned ligands for various signaling pathways. The hD_{2L} WT, S5.42A, S5.43A, and S5.46A receptors were expressed stably in CHO K1 cells and characterized by

TABLE 1

Competition binding data for [^{3}H]N-methylspiperone sites at TM5 serine mutants

Values represent mean ± S.E.M. The expression of these receptors was as follows: WT: K_D, 0.58 nM; B_{max}, 4.8 pmol/mg; S5.42A: K_D, 0.59 nM; B_{max}, 4.0 pmol/mg; S5.43A: K_D, 1.4 nM; B_{max}, 20.7 pmol/mg; S5.46A: K_D, 0.50 nM; B_{max}, 2.3 pmol/mg.

Mutant	$K_{0.5}$			
	WT	S5.42A	S5.43A	S5.46A
	nM			
DNS	144 ± 17	660 ± 190	750 ± 370	330 ± 160
DNX	83 ± 5	2700 ± 990*	770 ± 90	580 ± 340
DHX	490 ± 91	7400 ± 1000*	2,600 ± 50	1600 ± 40
Quinpirole	365 ± 6	1040 ± 100	27,000 ± 10,000*	2900 ± 820
Dopamine	450 ± 170	80,000 ± 3000*	31,000 ± 6000*	3500 ± 1,500

* Significantly different from WT ($P < 0.05$; one-way ANOVA and Tukey-Kramer Multiple Comparisons Test).
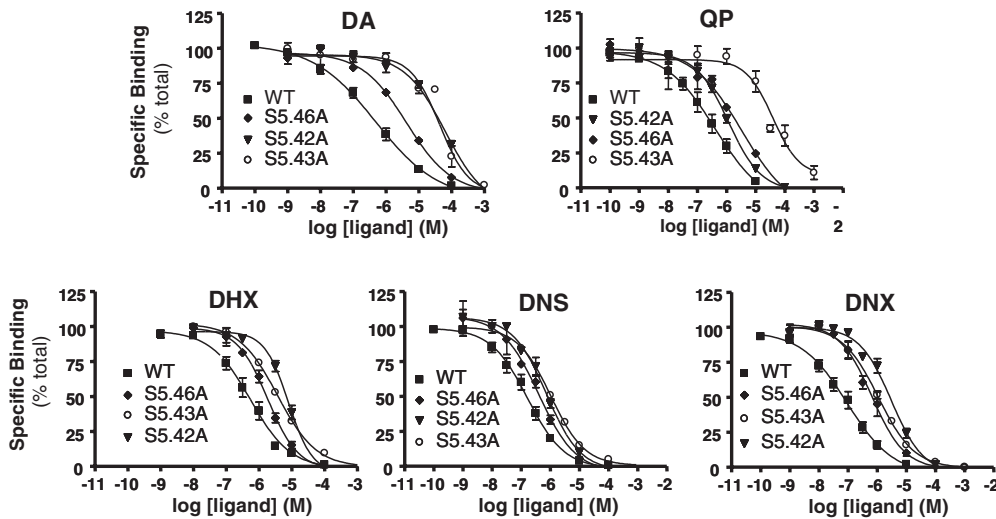
Fig. 2. Competition binding of test compounds with hD_{2L} WT and mutant receptors. Membranes were incubated with [^{3}H]N-methylspiperone as described under *Materials and Methods*. Analysis was conducted using nonlinear regression and a sigmoidal equation to determine IC_{50} values, reported as corrected affinity values ($K_{0.5}$). Assays were conducted in triplicate, and data represent three to four independent experiments. The mutations in the symbol key of each panel are listed in order of decreasing affinity.

means of saturation radioreceptor assays using [^{3}H]N-methylspiperone. As is shown in Table 1 and Supplementary Fig. 1, these mutations had only slight effects on the K_D, ranging from 0.50 nM for S5.46A to 1.4 nM for S5.43A (WT 0.58 nM). The expression level also was similar for the WT, S5.42A, and S5.46A (2.3–4.0 pmol/mg of protein), whereas the S5.43A expressed at a somewhat higher density (20.7 pmol/mg of protein).

Effect of S5.42A, S5.43A, and S5.46A on Affinity of Agonist Probe Ligands. The affinity for each probe ligand was determined using competition radioreceptor assays versus [^{3}H]N-methylspiperone in membranes from both WT and mutant receptors. An apparent affinity constant, $K_{0.5}$ (Table 1), was determined from experimental IC_{50} values corrected for radioligand K_D and concentration using the bimolecular Cheng-Prusoff relationship (Cheng and Prusoff, 1973). Competition binding studies also were conducted with several structurally distinct antagonists to rule out gross structural changes induced by the receptor (data not shown). Although all of the antagonists had slightly decreased affinity (as found for N-methylspiperone), the rank order of their affinity was unchanged, consistent with the hypothesis that these mutations caused no major changes to the overall receptor structure.

Representative data for each agonist probe ligand at each receptor are shown in Fig. 2 and summarized in Table 1. It should be noted that although the differences between drugs

was not always statistically significant when comparing the means (Table 1), the rank order was identical in each of the experimental replicates. The differential effects that these mutations had on the rigid probe ligands are striking. For example, the S5.42A and S5.46A mutations caused a much greater loss of affinity to DNX than to the structurally similar DNS. These differential changes can be seen by comparing the rank orders of affinity.

- WT: DNX > DNS > quinpirole = dopamine = DHX.
- S5.42A: DNS > quinpirole > DNX > DHX $\gg$ dopamine.
- S5.43A: DNS = DNX > DHX $\gg$ quinpirole = dopamine.
- S5.46A: DNS > DNX > DHX > quinpirole = dopamine.

Effect of Mutations on Ligand-Induced GtpγS Binding. An estimate of G protein turnover was conducted by assessing the ligand-induced binding of the nonhydrolyzable GTP analog [^{35}S]GTPγS (Fig. 3; Table 2). As has been reported previously (Gay et al., 2004), DHX and DNS were partial agonists at stimulating GTPγS binding, a property shared by DNX. The most remarkable finding in this experiment related to S5.43A. As noted above, this mutation caused a decrease in affinity of all of the ligands (Table 1; Fig. 2), yet the potency of the synthetic ligands in this assay was either unaffected or actually increased (significant for DNX). In addition, S5.43A actually increased the intrinsic activity of DNS. Conversely, S5.42A and S5.46A tended to cause a
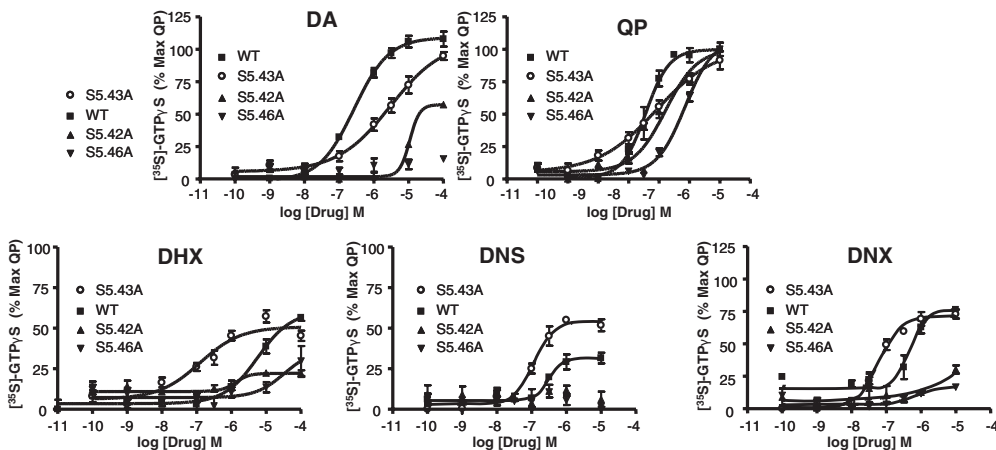

Fig. 3. GTPγS turnover experiments of test compounds with hD_{2L} WT and mutant receptors. Membrane fragments were incubated for 15 min with varying concentrations of test compounds until reaching equilibrium. 0.2 nM [^{35}S]GTPγS was then added for 30 min, and stimulation was measured. Quinpirole and dopamine had identical intrinsic activity in WT cells, and the actions of quinpirole were not affected by the mutations, hence all of the data regarding quinpirole activity in WT cells. Analysis was conducted using nonlinear regression and a sigmoidal equation to determine IC_{50} values reported in Table 2. Assays were conducted in triplicate and data represent three to four independent experiments. The mutations in the symbol key of each panel are listed in order of decreasing affinity.

TABLE 2
Potency of probe ligands in affecting GTPγS binding

Values represent $EC_{50} \pm$ S.E.M. for three to four independent experiments conducted in triplicate.

Mutant	EC_{50}			
	WT	S5.42A	S5.43A	S5.46A
	nM			
DNS	290 ± 70	—	135 ± 25	—
DNX	550 ± 30	—	69 ± 17*	660 ± 250
DHX	370 ± 180	1300 ± 410	92 ± 28	6600 ± 6200
Quinpirole	740 ± 120	1700 ± 860	203 ± 5	7200 ± 1900*
Dopamine	1700 ± 1040	10,700 ± 1500*	4300 ± 1600	—

* Significantly different from WT ($P < 0.05$; one-way ANOVA and Tukey-Kramer multiple comparisons test; —, potency cannot be measured because no functional activity was detected.

loss of both potency and intrinsic activity for all of the rigid ligands. Quinpirole was relatively unaffected; no change was evident in intrinsic activity and a significant decrease in potency occurred at only S5.46A.

Functional Biochemical Differences Caused by S5.42A. Measurement was conducted on the first of three D_2-linked pathways, agonist inhibition of forskolin-stimulated cAMP accumulation in a whole-cell assay system, for WT and S5.42A receptors (Fig. 4; Table 3; Supplemental Fig. 2). In the WT receptor, all dopamine agonists (DNS, DNX, DHX, quinpirole, and dopamine) robustly inhibited forskolin-stimulated cAMP accumulation. Conversely, inhibition of cAMP accumulation with the S5.42A mutant was abolished with all ligands tested except quinpirole. These data suggest that S5.42A is critical for ligand-receptor–mediated conformational changes associated with inhibitory actions of the D_{2L} receptor at cAMP accumulation (AC).

Measurement of a second pathway, agonist stimulation and subsequent phosphorylation of the p44/p42 MAP kinase, was then conducted in a whole-cell assay system for WT and S5.42A receptors (Fig. 4; Table 3; Supplemental Fig. 3). In

the WT receptor system, all dopamine agonists (DNS, DNX, DHX, quinpirole, and dopamine) fully activated MAPK. S5.42A only minimally affected the actions of quinpirole (EC_{50}, 44 nM) compared with WT (EC_{50}, 23 nM). Conversely, the S5.42A mutation caused a complete loss of function at this endpoint for DNS and DNX and a partial loss of intrinsic activity for DHX.

Measurement of a third pathway, agonist-stimulated [^{3}H]arachidonic acid release, was conducted in a whole-cell assay system for WT and S5.42A (Fig. 4; Table 3; Supplemental Fig. 4). The potency of quinpirole was decreased by the S5.42A mutation (EC_{50}, 223 versus 63 nM in WT), but intrinsic activity was unaffected. Conversely, all of the other ligands were inactive with the S5.42A receptor (see Table 3). The MAPK and AA functional data provide strong evidence that functional effects caused by the S5.42A mutation are ligand-dependent and do not represent a general dysfunction of the receptor.

Functional Biochemical Differences Caused by S5.43A Mutant. The hypothesis that Ser5.43 is critical for forming intrahelical H-bonds that stabilize the TM5 α helix

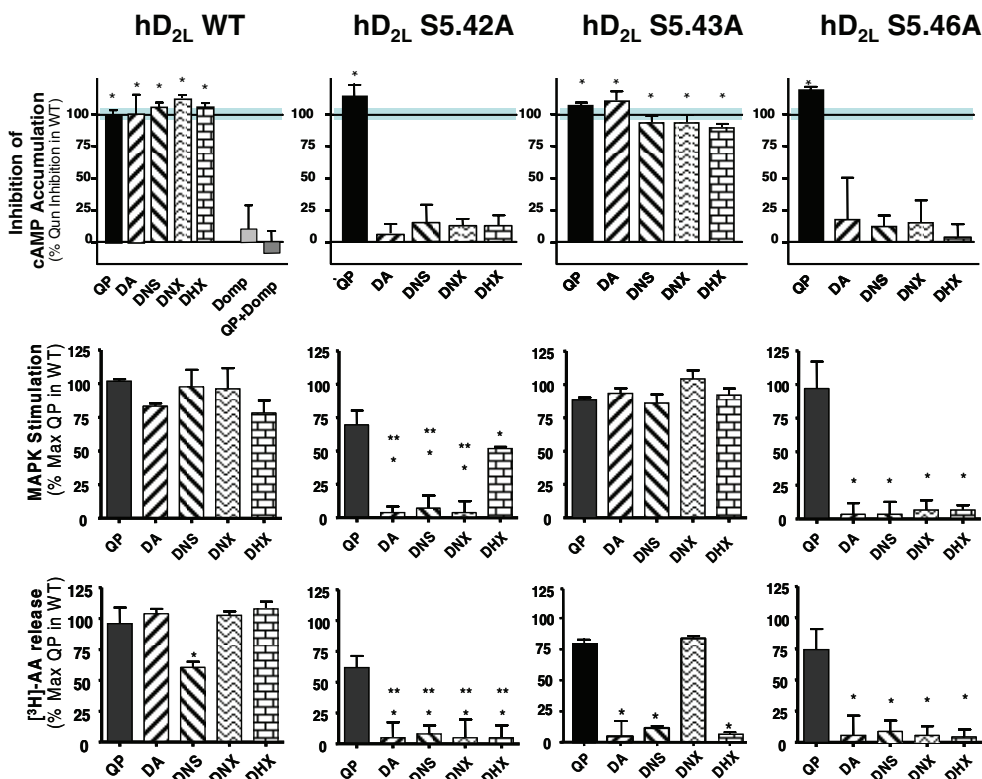## hD$_{2L}$ WT   hD$_{2L}$ S5.42A   hD$_{2L}$ S5.43A   hD$_{2L}$ S5.46A

Fig. 4. Ligand effects on intrinsic activity of second-messenger pathways of hD$_{2L}$ with mutations at S5.42A, S5.43A, and S5.46A. Top row, ligand-mediated inhibition of forskolin-stimulated cAMP accumulation (AC). [For the sake of comparison, in this panel, greater receptor-mediated inhibition is presented as a taller histogram bar when it actually represents greater inhibition.] Middle row, ligand-mediated activation of p44/p42 MAPK. Bottom row, ligand-mediated potentiation of [^{3}H]arachidonic acid release. Note that agonists inhibit AC but stimulate MAPK and AA release. Data are representative of E_{max} values for three to five independent experiments conducted in triplicate. *, $p < 0.05$ (one-way ANOVA, post hoc Dunnett's). **, $p < 0.05$ (Kruskal-Wallace one-way ANOVA, post hoc Dunn's).

TABLE 3
Effect of serine mutations on functional potencies of probe ligands
Values represent $EC_{50} \pm$ S.E.M. for three to four independent experiments conducted in triplicate.

Ligand	EC_{50}			
	WT	S5.42	S5.43A	S5.46
	nM			
Dopamine				
AC	46 ± 22	N.A.	$19 \pm 3*$	N.A.
MAPK	28 ± 7	N.A.	$114 \pm 40*$	N.A.
AA-release	49 ± 26	N.A.	N.A.	N.A.
Quinpirole				
AC	16 ± 6	7.8 ± 1.4	3 ± 1	54 ± 11
MAPK	26 ± 5	44 ± 12	26 ± 11	193 ± 28
AA-release	63 ± 12	$223 \pm 67*$	35 ± 27	$292 \pm 16*$
DNX				
AC	5.6 ± 0.3	N.A.	36 ± 17	N.A.
MAPK	27 ± 17	N.A.	$2,100 \pm 1,300$	N.A.
AA-release	101 ± 12	N.A.	$40 \pm 18*$	N.A.
DNS				
AC	193 ± 63	N.A.	119 ± 48	N.A.
MAPK	72 ± 68	N.A.	155 ± 9	N.A.
AA-release	340 ± 180	N.A.	N.A.	N.A.
DHX				
AC	93 ± 10	N.A.	125 ± 28	N.A.
MAPK	31 ± 105	69 ± 6.1	400 ± 130	N.A.
AA-release	395 ± 119	N.A.	N.A.	N.A.

N.A., no activity.
* Significantly different from WT ($P < 0.05$; one-way ANOVA and Tukey-Kramer multiple comparisons test).

was tested using functional profiling as summarized in Fig. 4 and Table 3. We hypothesized that mutation of S5.43A would have minimal effect on intrinsic activity at all endpoints measured with our test ligands. In support of that hypothesis, S5.43A had no effect on AC inhibition versus WT, although changes in rank order of potency were observed [WT: DNX > quinpirole > dopamine > DHX > DNS; S5.43A: quinpirole > dopamine > DNX > DNS > DHX (see Table 3 for EC_{50} values)].

The MAPK data are shown in Fig. 4, Table 3, and Supplemental Fig. 3. All of the test ligands (DNS, DNX, DHX, quinpirole, and dopamine) fully activated MAPK in both WT and the S5.43A mutant, although changes in rank order of potency were observed [WT: dopamine = quinpirole = DNX > DNS > DHX versus S5.43A: quinpirole > dopamine > DNS > DHX > DNX (see Table 3 for EC_{50} values)]. The S5.43A mutation had dramatic effects on agonist stimulated $[^3H]$arachidonic acid release (Fig. 4; Table 3; Supplemental Fig. 4). With the mutant receptor, quinpirole and DNX were minimally affected, but activity of the other ligands was lost. It is noteworthy that the structurally similar ligands DNS and DNX were affected oppositely with S5.43A. These data indicate that the effects of the S5.43A mutation were seen primarily on one function (AA), but not on two others (AC, MAPK), at which the full agonist activity at the WT receptor was maintained.

Functional Biochemical Differences Caused by S5.46A. Ser5.46 is the TM5 serine residue located deepest in the binding pocket of hD_{2L}. The S5.46A mutation did not affect the inhibition of AC by quinpirole, whereas none of the other ligands retained activity. In a similar fashion, at both MAPK and AA release, the activity of DNS, DNX, DHX, and dopamine were absent with the S5.46A mutant. Quinpirole maintained its intrinsic activity, but had modest loss of potency (5- to 8-fold) at both functions.

Discussion

The rigid ligands used here were developed as D_1 agonists but were previously shown also to be functionally selective D_2 ligands both in heterologous systems (Kilts et al., 2002; Gay et al., 2004) and in situ (Kilts et al., 2002; Mottola et al., 2002). They have atypical behavioral properties expected of canonical $D_1:D_2$ agonists (Darney et al., 1991; Smith et al., 1997; Gulwadi et al., 2001). Thus, these ligands provide useful probes for our studies, and resulting hypotheses may explain novel actions of these compounds in vivo.

Table 4 provides a nonquantitative summary of this study that will permit easier integration of these complex data. The S5.46A mutation caused a total loss of intrinsic activity for dopamine, dihydrexidine, dinapsoline, and dinoxyline but left quinpirole's intrinsic activity unaffected, suggesting that S5.46A did not disrupt the signaling ability. S5.43A mutation did not markedly affect the intrinsic activity of quinpirole at any function or affect the activity of DNX at any function, yet completely eliminated intrinsic activity for dopamine, dihydrexidine, and dinapsoline at AA release, but not other functions. Finally, S5.42A did not affect the intrinsic activity of quinpirole, but with one exception (DHX at MAPK) eliminated the intrinsic activity of dopamine and the rigid ligands. Functional selectivity also can be expressed as large and differential changes in potency (Gay et al., 2004) as shown in Table 4. A recent report showed that H6.55 mutations of the D_{2L} can abolish the bias of some functionally selective ligands (Tschammer et al., 2011), but the current study demonstrates that bias in a single function also can be introduced by a point mutation (Fig. 4).

Strengths and Weaknesses of this Experimental System. It is now realized that GPCR functional selectivity may not only involve differential activation of G protein heterotrimers, but also many other interactors (Urban et al., 2007). Thus, even in the same cell, the same receptor may be in-

TABLE 4
Qualitative summary of effects of mutations on probe ligands relative to WT.

Assay	DHX	DNS	DNX	QP	DA
S5.42A					
Binding	↓↓	↓	↓↓	↘	↓↓↓
GTPγS (EC$_{50}$)	↘	ID	ID	↔	↓
AC (EC$_{50}$)	ID	ID	ID	↑	ID
MAPK (EC$_{50}$)	↗	ID	ID	↔	ID
AA (EC$_{50}$)	ID	ID	ID	↘	ID
GTPγS (E$_{max}$)	↓↓	↓↓↓	↓↓	↔	↓↓
AC (E$_{max}$)	↓↓↓	↓↓↓	↓↓↓	↔	↓↓↓
MAPK (E$_{max}$)	↓↓	↓↓↓	↓↓↓	↓	↓↓↓
AA (E$_{max}$)	↓↓↓	↓↓↓	↓↓↓	↓↓	↓↓↓
S5.43A					
Binding	↓	↓	↓	↓↓↓	↓↓↓
GTPγS (EC$_{50}$)	↗	↗	↑	↗	↘
AC (EC$_{50}$)	↔	↔	↓	↓	↔
MAPK (EC$_{50}$)	↔	↔	↓↓↓	↔	↘
AA (EC$_{50}$)	ID	ID	↘	↘	ID
GTPγS (E$_{max}$)	↔	↑↑	↔	↔	↔
AC (E$_{max}$)	↔	↔	↔	↔	↔
MAPK (E$_{max}$)	↔	↔	↔	↔	↗
AA (E$_{max}$)	↓↓↓	↓↓↓	↓	↓	↓↓↓
S5.46A					
Binding	↔	↘	↓	↓	↓
GTPγS (EC$_{50}$)	↓↓	ID	↔	↓↓	↓
AC (EC$_{50}$)	ID	ID	ID	↗	↓
MAPK (EC$_{50}$)	ID	ID	ID	↓	↓
AA (EC$_{50}$)	ID	ID	ID	↓	↓
GTPγS (E$_{max}$)	↓↓	↓↓↓	↓↓↓	↔	↓↓↓
AC (E$_{max}$)	↓↓↓	↓↓↓	↓↓↓	↔	↓↓↓
MAPK (E$_{max}$)	↓↓↓	↓↓↓	↓↓↓	↔	↓↓↓
AA (E$_{max}$)	↓↓↓	↓↓↓	↓↓↓	↘	↓↓↓

↑, positive effect (i.e. decreased $K_{0.5}$, decreased EC$_{50}$, or increased E_{max}); ↔, minimal or no effect; ↓, detrimental effect (i.e. increased $K_{0.5}$, increased EC$_{50}$, or decreased E_{max}); ↘, trend downward; ↗, trend upward; ID, indeterminable. ↓ = 5- to 9-fold; ↓↓ = 10- to 50-fold; ↓↓↓ = >50-fold; QP, quinpirole.

volved in different "signalsomes," and a measured endpoint may be dependent on activity of two or more signalsomes. Although it may seem desirable to have a totally defined system in which to study different ligand-induced/stabilized states, this is technically difficult, and no available system recapitulates the characteristics seen consistently in situ and in single native cells.

Although we assume that mutation-induced functional selectivity is a consequence largely of alterations to the ligand-receptor interactions, it is possible that ligand-independent, mutation-induced alterations in the signalsome itself are involved. Two lines of evidence suggest this is not a major factor here. The reference ligand quinpirole has markedly different predicted docking poses compared with the D$_{2L}$ receptor. In our assays, quinpirole-induced functional activity was similar in mutant and WT receptors, suggesting that functionally selective signaling of rigid ligands is not due simply to disruption of D$_2$ signaling. Moreover, in the current studies, the effects on intrinsic activity were often dramatic (e.g., 100% or 0% intrinsic activity), but if differential changes were occurring via two alternate routes, partial agonism might have been expected.

This raises an ancillary point. The S5.43A line had a much higher receptor expression than the WT, S5.42A, or S5.46A lines (Table 1), suggesting that the failure to find partial agonism is a receptor reserve artifact. Yet partial agonism at GTPγS binding, uncorrelated with receptor expression, was seen for all three rigid ligands. Indeed, the high expressing S5.43A increased the potency of DNX in stimulating GTPγS binding, yet the same mutation markedly decreased DNX potency at adenylate cyclase. Thus, although receptor reserve may have influenced these results, the effect was prob-

ably minor. In the case of S5.43A, the mutation caused a major disruption only of a single function, and only for some ligands. Together, this suggests that the functional effects reflect alterations in ligand-receptor interactions and not gross disruption of receptor function.

Computational Analysis. As noted above, none of the mutations affected quinpirole activation, possibly because the full agonists (quinpirole, DA, DNS, DNX, and DHX) stabilize an ensemble of receptor conformations that show coupling affinities different from those of downstream proteins (Vaidehi and Kenakin, 2010). To test this hypothesis, we computed the binding energy (BE) landscapes of the agonists and D$_{2L}$ using the computational method of ligand-induced receptor conformational change that has been validated for prediction of activation of rhodopsin (Bhattacharya et al., 2008b) and β2-adrenergic receptor (Bhattacharya et al., 2008a; Bhattacharya and Vaidehi, 2010). As seen in Fig. 5C, the BE landscapes of dopamine shows two distinct minima (agonist states 1 and 2). The BE landscape of the other agonists are qualitatively similar (Supplemental Fig. 5). Small movements of TM3 and a counterclockwise rotation of TM5 (from the extracellular side) that brings Ser5.43 closer to the binding pocket characterize both minima. The difference between the two agonist-stabilized receptor conformations comes from TM6 movement. In receptor state 1, movement of TM6 brings His6.55 closer to TM5, whereas in state 2, TM6 movement brings His6.55 closer to TM7.

The agonist-preferred receptor conformations are stabilized by both interhelical and receptor-ligand contacts. Ser5.42 makes a hydrogen bond (HB) with the catechol hydroxyl groups of DA, DNS, and DNX (m-OH of DA, p-OH of DNS, DNX; Fig. 5, B and E) in both agonist states 1 and 2.
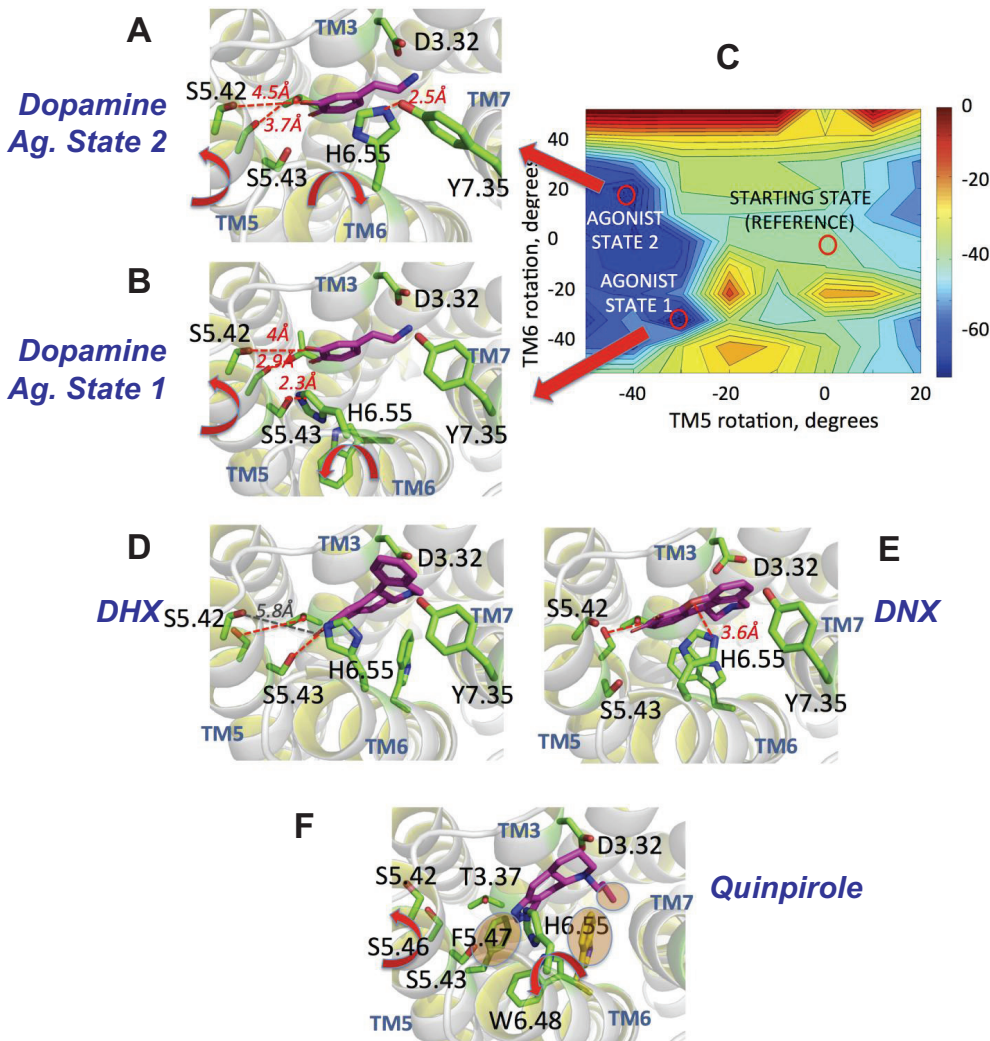
Fig. 5. Stabilization of multiple receptor conformations (agonist states 1 and 2) by the D_2 agonists. A, binding site of DA in agonist state 2; B, binding site of DA in agonist state 1; C, BE landscape of DA showing the different agonist stabilized states; D, binding site of DHX in agonist state 1; E, binding site of DNX in agonist state 1; F, binding site of quinpirole in agonist state 1. The red dotted lines represent HB contacts. In the quinpirole bound receptor, the moieties involved in stabilizing the active states are shaded.

This HB is missing in the DHX-bound structure (distance, 5.8Å), and therefore Ser5.42 contributes toward the stability of the receptor active states of DA, DNS, and DNX, but to a lesser extent for DHX. This is in agreement with the functional selectivity profile of the S5.42A mutant, which completely abolishes activation of all pathways for all the agonists except DHX and quinpirole, which still maintains partial activity toward the MAPK pathway. In conjunction with the predicted DHX bind site, this suggests that Ser5.42 does not form an HB with DHX in the MAPK-specific D_{2L} conformation. The lack of HB with Ser5.42 could be compensated by stronger HB of DHX with the other two serines or tighter aromatic contact between the agonist and the phenylalanines on TM5 and TM6. This is not clear, however, from the models. Thus, S5.42A has less drastic effect on DHX-mediated MAPK activation.

In contrast to Ser5.42, the effect of Ser5.43 is more pathway-specific. In the activation assays, the S5.43A mutant only affected the AA pathway, whereas the other two pathways were unaffected for all agonists. For the AA pathway, S5.43A abolished the intrinsic activity of DA, DNS, and DHX and retained partial activity for DNX and quinpirole. In our model, the receptor/agonist state 1 is stabilized by an HB between Ser5.43 and His6.55 (Fig. 5B). In contrast, the receptor/agonist state 2 is stabilized by the HB between

His6.55 and Tyr7.35 (Fig. 5A). Thus our model, in conjunction with the results from the S5.43A mutant, indicates that agonist state 1 may represent the receptor conformation that mediates AA activation, whereas slightly different agonist state 2 corresponds to the cAMP and MAPK activation, although this hypothesis will require further experimentation to test. In the DNX- and quinpirole-bound structures, the side chain of His6.55 is proximal to the ether oxygen of DNX and imidazole nitrogen of quinpirole, respectively. Thus, in the S5.43A mutant, DNX and quinpirole can stabilize agonist state 2 by forming HB with His6.55, whereas the other ligands (DA, DNS, DHX) that lack the polar motifs of DNX and quinpirole cannot form this HB and hence cannot stabilize state 1. These ligands require Ser5.43 to stabilize agonist state 1 and thus lose AA activity in the S5.43A mutant. This explains the insensitivity of S5.43A mutation toward DNX and quinpirole-mediated AA activation.

S5.46A eliminates activation of the three pathways for all agonists except quinpirole. In our agonist-stabilized model of the D_2 receptor, Ser5.46 forms a HB with Thr3.37 that stabilizes agonist states 1 and 2 (Fig. 5). Thus mutating Ser5.46 to Ala destabilizes both the active states and abolishes activity of all the three pathways. Among the agonists studied here, quinpirole shows a different activation profile compared with the rest of the agonists. In the experimental

activation assays, none of the serine mutations affected quinpirole-mediated D_2 activation. Unlike the catechol agonists, the nitrogen atoms on the imidazole of quinpirole are distant from the serine residues on TM5, precluding the strong HB with the serines in the agonist-stabilized states. This explains the insensitivity of the serine mutations toward quinpirole-mediated D_2 activation. To understand the mechanism of quinpirole activation, comparison of the interactions in the ligand-binding pockets in both the inactive and agonist-stabilized conformations showed that the *n*-propyl group of quinpirole is buried deep into the binding pocket, allowing direct contact with Trp6.48. The steric interaction could induce a change of rotamer of the Trp6.48 side chain, which in turn creates a steric clash with the side chain of Phe5.47 (Fig. 5F). To relieve the clash between Trp6.48 and Phe5.47, TM5 rotates counterclockwise, leading to the activation of the receptor. Thus, Trp6.48 and Phe5.47 form an aromatic switch that stabilizes the active states of quinpirole-bound hD_{2L}. Our model also suggests that His6.55 is important for quinpirole-mediated AA activation, because the HB between quinpirole and His6.55 contributes to the stability of agonist state 1.

Differences in the agonist stabilized receptor conformations could lead to functional selectivity in the D_{2L} receptor. Selective conformational stabilization by structurally distinct agonists was reported in β_2-adrenergic receptor (Ghanouni et al., 2001; Swaminath et al., 2005). Here we find that the three serine residues on TM5 interact differently with the agonist to stabilize distinct D_{2L} conformations for all agonists except quinpirole. The Ser5.46–Thr3.37 HB stabilizes the active state conformations of TM5, making Ser5.46 critical for all three activation pathways. In contrast, Ser5.43 stabilizes only one of the active states (AA pathway) by forming HB with His6.55. S5.42A shows different effects on the different agonists (less effect on DHX-MAPK activation) depending on the strength of the HB with various agonists. Besides the serines, the residue His6.55 is predicted to be important for the functionality of the D_2 receptor, and data to this effect were recently reported (Tschammer et al., 2011). In β-adrenergic receptors, the residue in the analogous position of His6.55 (Asn6.55) has been shown to be important for agonist activity. In the β_2-adrenergic receptor, the N6.55L mutation reduced the activity of norepinephrine (Wieland et al., 1996). In the agonist bound crystal structures of the β_1-adrenoreceptor (Warne et al., 2011), Asn6.55 forms an HB with Ser5.43 similar to the predicted agonist-bound structures of the D_2. In this work, His6.55 is predicted to stabilize the D_2 conformation responsible for AA activity by forming HB with Ser5.43 and polar groups of quinpirole and DNX. Unlike the serine mutations, which affect only the agonists with catechol motif, the H6.55A mutation is predicted to affect the activation of all agonists studied here, including quinpirole. The model of D_2 activation that emerges from this work is summarized in Fig. 6. Although the computational model presented here explains the differences between AA versus cAMP/MAPK pathways, we attribute changes in functional selectivity to ligand-receptor interactions, but neglects effects on receptor-protein interactors. Thus, functional selectivity can be engendered by mutations that perturb arrestin binding (Lan et al., 2009a; Lan et al., 2009b). Nonethe-
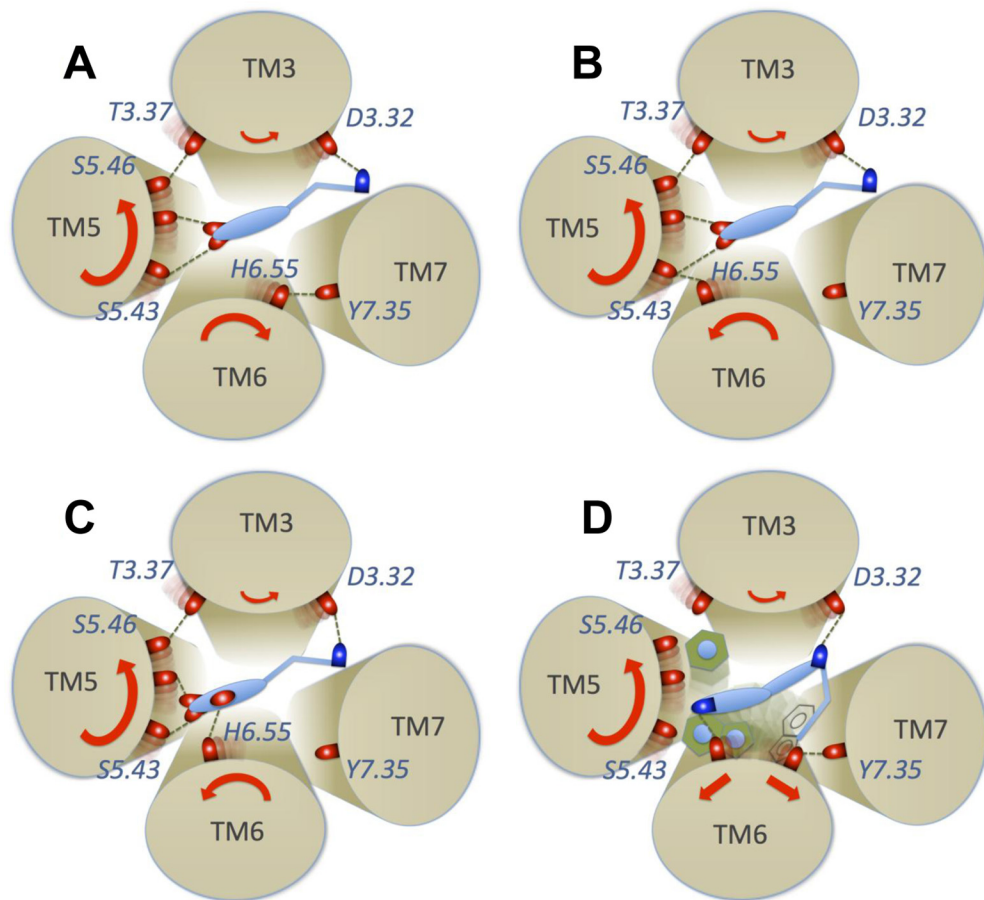

Fig. 6. Model of functional selectivity in hD_{2L}. The schematics show the receptor conformations corresponding to the different activation pathways stabilized by various agonists and the interhelical and receptor-ligand contacts looking from the extracellular side: A, cAMP/MAPK activation by ligands DA, DNS, DNX (agonist state 2 in Fig. 5). B, AA activation by DA, DHX, DNS (agonist state 1 in Fig. 5). C, AA activation by DNX. D, mechanism of activation by quinpirole for all three pathways. The orientation of TM6 where His6.55 faces TM5 corresponds to the AA pathway, whereas His6.55 facing TM7 represents cAMP/MAPK activation.

less, our data demonstrate that ligand-receptor interactions can be a determinant of signaling bias, and the one clearly most relevant to drug discovery.

Conclusions

Antagonists were essentially unaffected by these TM5 serine mutations because their binding to the D_2 receptor, unlike that of agonists, is less dependent on interactions with these residues. The effects on the binding of these agonist ligands also were largely predictable by existing molecular models, whereas these mutations caused patterns of effects on the functional activity of the probe ligands not directly predictable from binding. One hypothesis is that ligands can cause receptor populations to shift between groups of discrete active states that are linked to specific signaling pathways. Alternatively, each ligand may induce a discrete range of conformational changes that affect, in a graded fashion, whether specific signaling pathways are activated. At present, the former hypothesis is one that has been largely favored and is the one that would explain the constitutive activity often seen in cellular systems. In any event, the ability to form and test hypotheses about how such changes occur can be heuristically interesting but also may lead to structure-based discovery of novel functionally selective ligands.

Authorship Contributions

Participated in research design: Fowler, Bhattacharya, Vaidehi, and Mailman.

Conducted experiments: Fowler, Bhattacharya, and Urban.

Contributed new reagents or analytic tools: Fowler, Bhattacharya, and Vaidehi.

Performed data analysis: Fowler, Bhattacharya, Vaidehi, and Mailman.

Wrote or contributed to the writing of the manuscript: Fowler, Bhattacharya, Urban, Vaidehi, and Mailman.

References

Ballesteros JA and Weinstein H (1995) Integrated methods for the construction of three-dimensional models and computational probing of structure-function relations in G protein-coupled receptors. *Methods Neurosci* **25**:366–428.
Berg KA, Maayani S, Goldfarb J, Scaramellini C, Leff P, and Clarke WP (1998) Effector pathway-dependent relative efficacy at serotonin type 2A and 2C receptors: evidence for agonist-directed trafficking of receptor stimulus. *Mol Pharmacol* **54**:94–104.
Bhattacharya S, Hall SE, Li H, and Vaidehi N (2008a) Ligand-stabilized conformational states of human beta(2) adrenergic receptor: insight into G-protein-coupled receptor activation. *Biophys J* **94**:2027–2042.
Bhattacharya S, Hall SE, and Vaidehi N (2008b) Agonist-induced conformational changes in bovine rhodopsin: insight into activation of G-protein-coupled receptors. *J Mol Biol* **382**:539–555.
Bhattacharya S, Subramanian G, Hall S, Lin J, Laoui A, and Vaidehi N (2010) Allosteric antagonist binding sites in class B GPCRs: corticotropin receptor 1. *J Comput Aided Mol Des* **24**:659–674.
Bhattacharya S and Vaidehi N (2010) Computational mapping of the conformational transitions in agonist selective pathways of a G-protein coupled receptor. *J Am Chem Soc* **132**:5205–5214.
Brewster WK, Nichols DE, Riggs RM, Mottola DM, Lovenberg TW, Lewis MH, and Mailman RB (1990) *trans*-10,11-dihydroxy-5,6,6a,7,8,12b-hexahydrobenzo[a]phenanthridine: a highly potent selective dopamine D1 full agonist. *J Med Chem* **33**:1756–1764.
Brown JT, Kant A, and Mailman RB (2009) Rapid, semi-automated, and inexpensive radioimmunoassay of cAMP: application in GPCR-mediated adenylate cyclase assays. *J Neurosci Methods* **177**:261–266.
Canutescu AA and Dunbrack RL, Jr. (2003) Cyclic coordinate descent: A robotics algorithm for protein loop closure. *Protein Sci* **12**:963–972.

Charifson PS, Bowen JP, Wyrick SD, Hoffman AJ, Cory M, McPhail AT, and Mailman RB (1989) Conformational analysis and molecular modeling of 1-phenyl-, 4-phenyl-, and 1-benzyl-1,2,3,4-tetrahydroisoquinolines as D_1 dopamine receptor ligands. *J Med Chem* **32**:2050–2058.
Cheng Y and Prusoff WH (1973) Relationship between the inhibition constant (K1) and the concentration of inhibitor which causes 50 per cent inhibition (I50) of an enzymatic reaction. *Biochem Pharmacol* **22**:3099–3108.
Cox BA, Henningsen RA, Spanoyannis A, Neve RL, and Neve KA (1992) Contributions of conserved serine residues to the interactions of ligands with dopamine D_2 receptors. *J Neurochem* **59**:627–635.
Darney KJ Jr, Lewis MH, Brewster WK, Nichols DE, and Mailman RB (1991) Behavioral effects in the rat of dihydrexidine, a high-potency, full-efficacy D1 dopamine receptor agonist. *Neuropsychopharmacology* **5**:187–195.
Fiser A and Sali A (2003) Modeller: generation and refinement of homology-based protein structure models. *Methods Enzymol* **374**:461–491.
Gay EA, Urban JD, Nichols DE, Oxford GS, and Mailman RB (2004) Functional selectivity of D2 receptor ligands in a Chinese hamster ovary hD2L cell line: evidence for induction of ligand-specific receptor states. *Mol Pharmacol* **66**:97–105.
Ghanouni P, Gryczynski Z, Steenhuis JJ, Lee TW, Farrens DL, Lakowicz JR, and Kobilka BK (2001) Functionally different agonists induce distinct conformations in the G protein coupling domain of the beta 2 adrenergic receptor. *J Biol Chem* **276**:24433–24436.
Ghosh D, Snyder SE, Watts VJ, Mailman RB, and Nichols DE (1996) 9-Dihydroxy-2,3,7,11b-tetrahydro-1H-naph[1,2,3-de]isoquinoline: a potent full dopamine D1 agonist containing a rigid-beta-phenyldopamine pharmacophore. *J Med Chem* **39**:549–555.
Grubbs RA, Lewis MM, Owens-Vance C, Gay EA, Jassen AK, Mailman RB, and Nichols DE (2004) 8,9-dihydroxy-1,2,3,11b-tetrahydrochromeno[4,3,2,-de]isoquinoline (dinoxyline), a high affinity and potent agonist at all dopamine receptor isoforms. *Bioorg Med Chem* **12**:1403–1412.
Gulwadi AG, Korpinen CD, Mailman RB, Nichols DE, Sit SY, and Taber MT (2001) Dinapsoline: characterization of a D_1 dopamine receptor agonist in a rat model of Parkinson's disease. *J Pharmacol Exp Ther* **296**:338–344.
Harper JF and Brooker G (1975) Femtomole sensitive radioimmunoassay for cyclic AMP and cyclic GMP after 2′0 acetylation by acetic anhydride in aqueous solution. *J Cyclic Nucleotide Res* **1**:207–218.
Kenakin T (1995) Agonist-receptor efficacy. II. Agonist trafficking of receptor signals. *Trends Pharmacol Sci* **16**:232–238.
Kenakin TP (2007) Functional Selectivity through Protean and Biased Agonism:Who Steers the Ship? *Mol Pharmacol*.
Kilts JD, Connery HS, Arrington EG, Lewis MM, Lawler CP, Oxford GS, O'Malley KL, Todd RD, Blake BL, Nichols DE, et al. (2002) Functional selectivity of dopamine receptor agonists. II. Actions of dihydrexidine in D2L receptor-transfected MN9D cells and pituitary lactotrophs. *J Pharmacol Exp Ther* **301**:1179–1189.
Lan H, Liu Y, Bell MI, Gurevich VV, and Neve KA (2009a) A dopamine D2 receptor mutant capable of G protein-mediated signaling but deficient in arrestin binding. *Mol Pharmacol* **75**:113–123.
Lan H, Teeter MM, Gurevich VV, and Neve KA (2009b) An intracellular loop 2 amino acid residue determines differential binding of arrestin to the dopamine D2 and D3 receptors. *Mol Pharmacol* **75**:19–26.
Lawler CP, Prioleau C, Lewis MM, Mak C, Jiang D, Schetz JA, Gonzalez AM, Sibley DR, and Mailman RB (1999) Interactions of the novel antipsychotic aripiprazole (OPC-14597) with dopamine and serotonin receptor subtypes. *Neuropsychopharmacology* **20**:612–627.
Lawler CP, Watts VJ, Booth RG, Southerland SB, and Mailman RB (1994) Discrete functional selectivity of drugs: OPC-14597. A selective antagonist for post-synaptic dopamine D2 receptors (Abstract). *Soc Neurosci Abstr* **20**:525.
Lovenberg TW, Brewster WK, Mottola DM, Lee RC, Riggs RM, Nichols DE, Lewis MH, and Mailman RB (1989) Dihydrexidine, a novel selective high potency full dopamine D-1 receptor agonist. *Eur J Pharmacol* **166**:111–113.
Mailman RB (2007) GPCR functional selectivity has therapeutic impact. *Trends Pharmacol Sci* **28**:390–396.
Mansour A, Meng F, Meador-Woodruff JH, Taylor LP, Civelli O, and Akil H (1992) Site-directed mutagenesis of the human dopamine D_2 receptor. *Eur J Pharmacol* **227**:205–214.
McDonald IK and Thornton JM (1994) Satisfying hydrogen bonding potential in proteins. *J Mol Biol* **238**:777–793.
Milligan G (1999) *Signal Transduction: A Practical Approach,* Oxford University Press, New York.
Mottola DM, Cook LL, Jones SR, Booth RG, Nichols DE, and Mailman RB (1991) Dihydrexidine, a selective dopamine receptor agonist that may discriminate postsynaptic D_2 receptors (Abstract). *Soc Neurosci Abstr* **17**:818.
Mottola DM, Kilts JD, Lewis MM, Connery HS, Walker QD, Jones SR, Booth RG, Hyslop DK, Piercey M, Wightman RM, et al. (2002) Functional selectivity of dopamine receptor agonists. I. Selective activation of postsynaptic dopamine D2 receptors linked to adenylate cyclase. *J Pharmacol Exp Ther* **301**:1166–1178.
Mottola DM, Laiter S, Watts VJ, Tropsha A, Wyrick SD, Nichols DE, and Mailman RB (1996) Conformational analysis of D1 dopamine receptor agonists: pharmacophore assessment and receptor mapping. *J Med Chem* **39**:285–296.
Neve KA (2009) *Functional Selectivity of G Protein-Coupled Receptor Ligands,* Humana Press, New York.
Nichols DE (1983) The development of novel dopamine agonists, in *Dopamine Receptors* (Kaiser C and Kebabian JW eds) pp 201–218, American Chemical Society, Washington DC.
Ryman-Rasmussen JP, Nichols DE, and Mailman RB (2005) Differential activation of adenylate cyclase and receptor internalization by novel dopamine D1 receptor agonists. *Mol Pharmacol* **68**:1039–1048.
Shapiro DA, Renock S, Arrington E, Chiodo LA, Liu LX, Sibley DR, Roth BL, and Mailman R (2003) Aripiprazole, a novel atypical antipsychotic drug with a unique and robust pharmacology. *Neuropsychopharmacology* **28**:1400–1411.

Shi L and Javitch JA (2002) The binding site of aminergic G protein-coupled receptors: the transmembrane segments and second extracellular loop. *Annu Rev Pharmacol Toxicol* **42**:437–467.

Smith HP, Nichols DE, Mailman RB, and Lawler CP (1997) Locomotor inhibition, yawning and vacuous chewing induced by a novel dopamine D2 post-synaptic receptor agonist. *Eur J Pharmacol* **323**:27–36.

Strader CD, Candelore MR, Hill WS, Sigal IS, and Dixon RA (1989) Identification of two serine residues involved in agonist activation of the beta-adrenergic receptor. *J Biol Chem* **264**:13572–13578.

Swaminath G, Deupi X, Lee TW, Zhu W, Thian FS, Kobilka TS, and Kobilka B (2005) Probing the beta2 adrenoceptor binding site with catechol reveals differences in binding and activation by agonists and partial agonists. *J Biol Chem* **280**:22165–22171.

Tschammer N, Bollinger S, Kenakin T, and Gmeiner P (2011) Histidine 6.55 is a major determinant of ligand-biased signaling in dopamine D2L receptor. *Mol Pharmacol* **79**:575–585.

Urban JD, Clarke WP, von Zastrow M, Nichols DE, Kobilka B, Weinstein H, Javitch JA, Roth BL, Christopoulos A, Sexton PM, et al. (2007) Functional selectivity and classical concepts of quantitative pharmacology. *J Pharmacol Exp Ther* **320**:1–13.

Vaidehi N and Kenakin T (2010) The role of conformational ensembles of seven transmembrane receptors in functional selectivity. *Curr Opin Pharmacol* **10**:775–781.

Versteeg HH, Nijhuis E, van den Brink GR, Evertzen M, Pynaert GN, van Deventer SJ, Coffer PJ, and Peppelenbosch MP (2000) A new phosphospecific cell-based ELISA for p42/p44 mitogen-activated protein kinase (MAPK), p38 MAPK, protein kinase B and cAMP-response-element-binding protein. *Biochem J* **350**:717–722.

Warne T, Moukhametzianov R, Baker JG, Nehmé R, Edwards PC, Leslie AG, Schertler GF, and Tate CG (2011) The structural basis for agonist and partial agonist action on a beta(1)-adrenergic receptor. *Nature* **469**:241–244.

Wieland K, Zuurmond HM, Krasel C, IJzerman AP, and Lohse MJ (1996) Involvement of Asn-293 in stereospecific agonist recognition and in activation of the beta 2-adrenergic receptor. *Proc Natl Acad Sci USA* **93**:9276–9281.

Wiens BL, Nelson CS, and Neve KA (1998) Contribution of serine residues to constitutive and agonist-induced signaling via the D2S dopamine receptor: evidence for multiple, agonist-specific active conformations. *Mol Pharmacol* **54**:435–444.

Woodward R, Coley C, Daniell S, Naylor LH, and Strange PG (1996) Investigation of the role of conserved serine residues in the long form of the rat D2 dopamine receptor using site-directed mutagenesis. *J Neurochem* **66**:394–402.

Zamanakos G (2001) A fast and accurate analytic method for the computation of solvent effects in molecular simulations. PhD dissertation, California Institute of Technology, Pasadena, CA.

Address correspondence to: Dr. Richard B. Mailman, Penn State University College of Medicine - Milton S. Hershey Medical Center, Department of Pharmacology. R130, 500 University Dr., P.O. Box 850, Hershey PA 17033-0850. E-mail: rmailman@psu.edu